Journal of
Applied
Crystallography

ISSN 0021-8898

Received 19 May 2003
Accepted 27 October 2003

Thermal expansion and crystal structure of cementite, Fe_3C, between 4 and 600 K determined by time-of-flight neutron powder diffraction

I. G. Wood,[a]* Lidunka Vočadlo,[a] K. S. Knight,[b,c] David P. Dobson,[a]‡ W. G. Marshall,[b] G. David Price[a] and John Brodholt[a]

[a]Department of Earth Sciences, University College London, Gower Street, London WC1E 6BT, UK, [b]ISIS Facility, Rutherford Appleton Laboratory, Chilton, Didcot, Oxon OX11 0QX, UK, and [c]Department of Mineralogy, The Natural History Museum, Cromwell Road, London SW7 5BD, UK. Correspondence e-mail: ian.wood@ucl.ac.uk

The cementite phase of Fe_3C has been studied by high-resolution neutron powder diffraction at 4.2 K and at 20 K intervals between 20 and 600 K. The crystal structure remains orthorhombic (*Pnma*) throughout, with the fractional coordinates of all atoms varying only slightly (the magnetic structure of the ferromagnetic phase could not be determined). The ferromagnetic phase transition, with $T_c \simeq 480$ K, greatly affects the thermal expansion coefficient of the material. The average volumetric coefficient of thermal expansion above T_c was found to be 4.1 (1) $\times 10^{-5}$ K^{-1}; below T_c it is considerably lower ($< 1.8 \times 10^{-5}$ K^{-1}) and varies greatly with temperature. The behaviour of the volume over the full temperature range of the experiment may be modelled by a third-order Grüneisen approximation to the zero-pressure equation of state, combined with a magnetostrictive correction based on mean-field theory.

1. Introduction

The physical properties of the cementite phase of Fe_3C have been of interest to Earth and planetary scientists since it was suggested (Wood, 1993) that they were consistent with those of the Earth's inner core. Two very recent studies of the ambient-temperature equation of state of this material (Scott *et al.*, 2001; Li *et al.*, 2002) have been made using high-pressure X-ray powder diffraction with diamond-anvil cells. The results obtained for the incompressibility, K_o, and its first derivative with respect to pressure, K_o', from these two experiments are in almost exact agreement ($K_o = 175 \pm 4$ GPa, $K_o' = 5.2 \pm 0.3$ and $K_o = 174 \pm 6$ GPa, $K_o' = 4.8 \pm 0.8$) and are very close to the values assumed by Wood (1993). At first sight, it might, therefore, be concluded that the case for Fe_3C as a major component of the inner core has been significantly strengthened by these measurements. However, a recent first-principles computer simulation study, combined with preliminary measurements of the thermal expansion of Fe_3C above room temperature by neutron powder diffraction (Vočadlo, Brodholt *et al.*, 2002), has cast doubt on these conclusions and, indeed, has suggested that the physical properties of Fe_3C are not compatible with those of the inner core as determined from seismology. At room temperature, Fe_3C is a metallic ferromagnet, with the transition to the paramagnetic state occurring at a Curie temperature, T_c, of about 483 K (*e.g.* Tsuzuki *et al.*, 1984). The neutron diffraction experiments showed that this magnetic phase transition had a significant effect on the volumetric thermal expansion coefficient, which was found to be, for example, $\sim 1.3 \times 10^{-5}$ K^{-1} at 300 K but $\sim 4.3 \times 10^{-5}$ K^{-1} for $T > T_c$. Similarly, the computer simulations showed that the ferromagnetic ordering greatly affected the values of the parameters needed to define the equation of state; calculations for the magnetically ordered phase led to values of K_o and K_o' in good agreement with those of Scott *et al.* (2001) and Li *et al.* (2002), whereas 'non-magnetic' calculations (in which the occupation numbers of every electron orbital were forced to be equal for up and down spins) gave a much higher incompressibility (~316 GPa) offset by a much lower value for the volume at zero pressure. As expected, the calculations predicted a transition to a high-pressure non-magnetically ordered state with $P_c \simeq 60$ GPa. Under the conditions that exist in the Earth's inner core, Fe_3C will not be magnetically ordered; determinations of the equation of state of its ferromagnetic phase are, therefore, of doubtful value in discussing its possible significance in the inner core.

The cementite structure of Fe_3C (termed cohenite in its mineral form) is orthorhombic, space group *Pnma*, with $Z = 4$. The structure (Herbstein & Smuts, 1964; Fasiska & Jeffrey, 1965) can be viewed either in terms of pleated layers of Fe atoms, derived from a hexagonal close packed (h.c.p.) structure, with C atoms occupying interstitial sites (Fasiska & Jeffrey, 1965; Hyde & Andersson, 1989), or as being isostructural with YF_3 (Hyde & Andersson, 1989) and hence derived from the $GdFeO_3$ orthorhombic perovskite structure with the octahedral cations absent. As indicated above, at

‡ Formerly at Bayerisches Geoinstut, Universität Bayreuth, D-95440 Bayreuth, Germany.

room pressure and temperature the material is metallic and ferromagnetically ordered (Hofer & Cohn, 1959; Tsuzuki *et al.*, 1984; Häglund *et al.*, 1991). Neither the magnetic structure nor the direction of spontaneous magnetization appear to have been determined. Previous thermal expansion measurements have been made by Gachon & Schmitt (1971) and by Reed & Root (1998). Gachon & Schmitt (1971) used X-ray powder diffraction in the range 73–773 K; however, they made measurements at only five different temperatures and so their thermal expansion curves were insufficiently sampled to reveal any effects arising from the ferromagnetic transition. In the study by Reed & Root (1998), cell parameters were determined only above the ferromagnetic transition (from 523 K to 1073 K), by angle-dispersive neutron powder diffraction using a large multi-phase ingot formed from a mixture of Fe with 2.77 wt% C. The maximum amount of cementite that might be produced in this way would correspond to 45 wt% of the final sample, the remainder being principally ferrite (*i.e.* α-Fe with some interstitial carbon) or austenite (*i.e.* γ-Fe with interstitial carbon) depending upon the sample temperature. The behaviour of the material was reported to change at about 873 K, where it showed a rather abrupt increase in the thermal expansion coefficient of the *b* axis, combined with a corresponding decrease in the expansion coefficients for *a* and *c*, such that the net volumetric expansion coefficient remained unchanged.

In the present paper, we describe a detailed study of the thermal expansion of Fe_3C from 4.2 K to 600 K by high-resolution neutron powder diffraction. In our previous preliminary study of this material, using the POLARIS diffractometer at ISIS, we had examined the material only above room temperature and these data were insufficient to study the effects of the ferromagnetic transition in any detail. In this earlier work, we had attempted to extend the measurements to higher temperatures. We found, however, that the material started slowly to decompose, producing α-iron, above about 650 K, with rapid decomposition occurring above 800 K, and it was, therefore, decided to limit the present study to temperatures below 600 K. It is of interest to note that we observed decomposition of Fe_3C to occur at temperatures very much lower than those quoted by Tsuzuki *et al.* (1984), who stated that it dissociated under N_2 gas (to give α-iron and carbon) only above 973 K; we attribute this difference to the much longer duration of our experiment and to the fact that the sample was under high vacuum within the furnace.

2. Experimental details

The sample used was prepared from mixtures of 90 wt% Fe and 10 wt% C (*i.e.* containing an excess of carbon over the 6.7 wt% required for stoichiometry), following the procedure of Tsuzuki *et al.* (1984). The mixtures were pelleted under 50 MPa pressure and packed in Pyrex glass tubes with graphite end caps, which were then loaded into 3/4-inch talc–Pyrex piston–cylinder assemblies and sintered at 1.5 GPa and 1473–1523 K for 30 min. Each synthesis experiment yielded approximately 0.85 g of Fe_3C with a small excess of graphite. The Fe_3C was separated by firstly removing any large pieces of graphite adhering to the ends of the sample with a scalpel and tweezers. After this, the material was crushed and ground by hand under acetone using an agate pestle and mortar. Final separation of the Fe_3C was then made by a combination of magnetic separation and removal of the more-slowly-settling component when the sample was suspended in acetone, shaken and ultrasonically agitated. Examination by X-ray powder diffraction, using a computer-controlled Philips PW 1050 vertical goniometer with Fe-filtered Co $K\alpha$ radiation, revealed three small impurity peaks, the strongest of which had a peak height of approximately 2.5% that of the strongest peak from Fe_3C; these had *d* spacings of approximately 2.49, 2.16 and 1.53 Å, which correspond to the three strongest reflections from wüstite (FeO).

The sample used for neutron diffraction was made by combining three batches of material prepared as described above, to give a total sample mass of approximately 1.3 g. Time-of-flight neutron powder diffraction patterns were collected using the high-resolution powder diffractometer (HRPD) (Ibberson *et al.*, 1992) at the ISIS spallation neutron source of the Rutherford Appleton Laboratory (RAL). The sample environment was controlled using the ISIS facility's 'cryofurnace', with the powder sample, loosely packed in a rectangular aluminium sample can, held under a partial pressure of 30 mbar of He exchange gas. A rhodium–iron resistance thermometer was used to measure the temperature, which was controlled to better than ± 0.1 K during the data collection. Diffraction patterns were collected with flight times from 50–150 ms, using both the backscattering ($2\theta \simeq 168^\circ$) and perpendicular ($2\theta \simeq 90^\circ$) detector banks, corresponding to *d* spacings of 1.04–3.11 Å and 1.45–4.35 Å, respectively. The temperature range covered corresponded to the maximum accessible with the cryofurnace, with data collected at 4.2 K (counting for 2 h) and then, on heating, in 20 K steps from 20 to 600 K (counting for 1 h at each temperature point).

The cell parameters were obtained by profile refinement of the backscattering data using the *CAILS* ('cell and intensity least squares') refinement technique (after Pawley, 1981) implemented in RAL's suite of programs based on the *Cambridge Crystallography Subroutine Library* (*CCSL*; Brown & Matthewman, 1993). It was felt that this technique, which requires no knowledge of the crystal (or magnetic) structure other than the space group, would give the least biased and most precise estimate of the unit cell. The crystal structures were then refined using the Rietveld method implemented in the program *GSAS* (Larson & Von Dreele, 1994), fitting the model simultaneously to both the 90° and the backscattering data over the ranges $1.51 \leq d \leq 4.06$ Å and $1.08 \leq d \leq 2.90$ Å, respectively. The magnetic contribution to the scattering was ignored (as discussed below), as was the contribution from the impurity phase; apart from a small peak at 2.16 Å (from the vanadium windows and heat shields, see Fig. 1), no obvious features in the $(y_{obs} - y_{calc})$ difference pattern were observed that could be attributed to neglect of these terms. However, in view of the possible effect of the neglect of the magnetic scattering on the refined values of

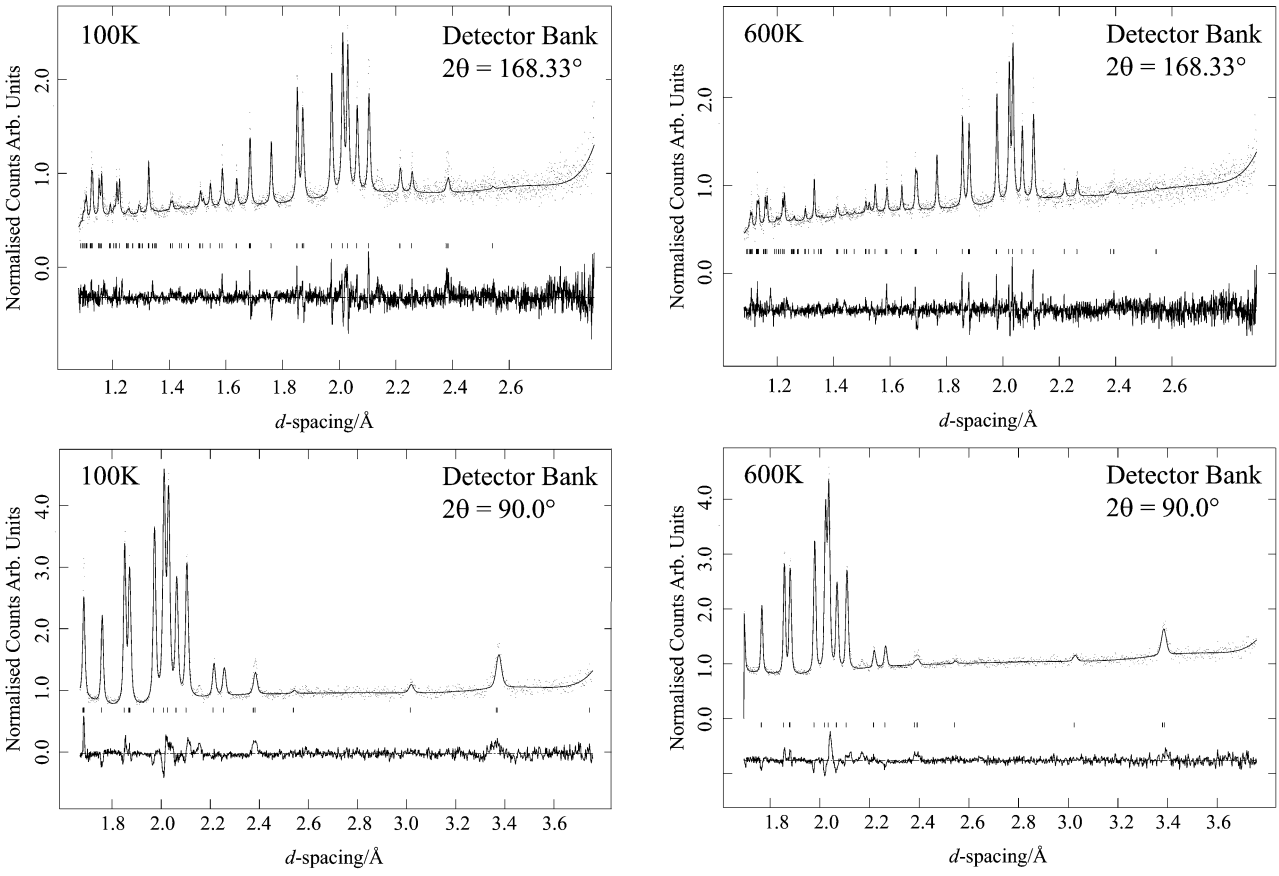

Figure 1
Neutron powder diffraction patterns of Fe_3C at 100 K (ferromagnetic phase) and 600 K (paramagnetic phase). Experimental data are shown as points, the line giving the calculated pattern from the Rietveld refinement. The lower trace shows the difference between the observed and calculated values and the tick marks give the expected positions of the Bragg reflections. The 2θ values shown (168° and 90°) refer to the scattering angles of the HRPD detector banks.

atomic displacement parameters and the rather poor counting statistics of the data (resulting from the limited quantity of sample available), it was decided that the use of anisotropic displacement parameters could not be justified; it was also decided to constrain the isotropic displacement parameters of the two Fe atoms to be equal. 36 variables were, therefore, included in the Rietveld refinements (two scale factors, two profile parameters, ten background coefficients for each of the two data sets, three cell parameters, seven fractional coordinates and two atomic displacement parameters). The values of χ^2 were in the range 1.5–2 throughout, for approximately 4450 profile points (the value of χ^2 at 4.2 K is a little higher, 3.1, as the counting statistics for this data set are better), with corresponding weighted profile (R_{wp}) and profile (R_p) R factors in the ranges 6–7% and 5–6%, respectively. Representative diffraction patterns at 100 K (ferromagnetic phase) and 600 K (paramagnetic phase) are shown in Fig. 1.

3. Results and discussion

3.1. Lattice parameters and thermal expansion

Fig. 2 shows the orthorhombic cell parameters as a function of temperature. It is clear that the magnetic transition greatly affects the thermal expansion coefficients of the material. Initial inspection of Fig. 2 suggests that the three axes behave rather differently from one another. The effect of the ferromagnetic transition on the a axis seems especially pronounced, with this direction showing a negative thermal expansion coefficient for all temperatures below T_c, whereas the behaviours of the b and c axes are somewhat similar, with the effect of the magnetic transition contributing relatively more to the form of the overall thermal expansion in the case of the c axis. However, if the cell parameters of the paramagnetic phase are extrapolated to 0 K, it becomes apparent that the excess length arising from the magnetic ordering is ~0.02 Å for all three axes. The differences seen in Fig. 2, therefore, primarily reflect the different relative magnitudes of the magnetostrictive and vibrational contributions to the expansion in each case.

The unit-cell volume as a function of temperature is shown in Fig. 3(a), with the volumetric thermal expansion coefficient given in Fig. 3(b). As expected from the results shown in Figs. 2 and 3(a), the expansion coefficient in the ferromagnetic phase varies greatly with temperature, approaching zero close to T_c as well as at 0 K (where this value is required by thermodynamics). In addition, however, it appears that the expansion coefficient of the paramagnetic phase above T_c is

also strongly temperature dependent, at least for the temperature interval covered in this experiment. Similar behaviour is observed, for example, in α-iron (Kohlhaas *et al.*, 1967), associated with the ferromagnetic phase transition at about 1045 K. This competition between the thermal expansion arising from vibrations of the atoms and the increase in volume with decreasing temperature arising from spontaneous magnetostriction provides the basis for the family of 'Invar' alloys (such as Fe with 36 wt% Ni), which have very low thermal expansion around room temperature.

Current studies of Fe_3C are mainly concerned with its possible occurrence in the Earth's core; it is, therefore, its physical properties in a high-pressure 'non-magnetic' state (with Pauli paramagnetism but in which there are no local magnetic moments on the atoms) that are of most interest to Earth scientists. Such a phase only exists above ~60 GPa (Vočadlo, Brodholt *et al.*, 2002) and is therefore not readily accessible experimentally. The accessible high-temperature paramagnetic phase (in which there are local magnetic moments but they are randomly disordered) will, however, be more representative of the core-forming phase than the ferromagnetically ordered material (for further discussion see below). To determine the thermal expansion coefficient of this phase in the form tabulated by Fei (1995), the eight data points shown in Fig. 2 for which $T \geq 460$ K were fitted to

$$V(T) = V_{T_r} \exp\left[\int_{T_r}^{T} \alpha(T)\,\mathrm{d}T\right], \tag{1}$$

where V_{T_r} is the volume at a chosen reference temperature, T_r, and $\alpha(T)$ is the thermal expansion coefficient, having the form

$$\alpha(T) = a_o + a_1 T. \tag{2}$$

This fit gave values of $V_{T_r} = 154.8\,(1)$ Å^3, $a_o = -4\,(2) \times 10^{-5}$ K^{-1} and $a_1 = 1.6\,(3) \times 10^{-7}$ K^{-2}, for a chosen T_r of 300 K. The large standard uncertainties in a_o and a_1 arise from the limited temperature range and the small number of data points available. The form of these parameters, with a_o negative and a_1 strongly positive, reflects the strong temperature dependence of α seen in the data, but probably also implies that it would be unwise to use them to extrapolate α to much higher temperatures. Expressed in this way, α takes values of $3\,(2) \times 10^{-5}$ K^{-1} at 460 K and $6\,(3) \times 10^{-5}$ K^{-1} at 600 K, in good agreement with the results of Reed & Root (1998) from which a temperature-independent value of $5.2\,(2) \times 10^{-5}$ K^{-1} can be derived [defined as $\alpha = (1/V)(\mathrm{d}V/\mathrm{d}T)$].

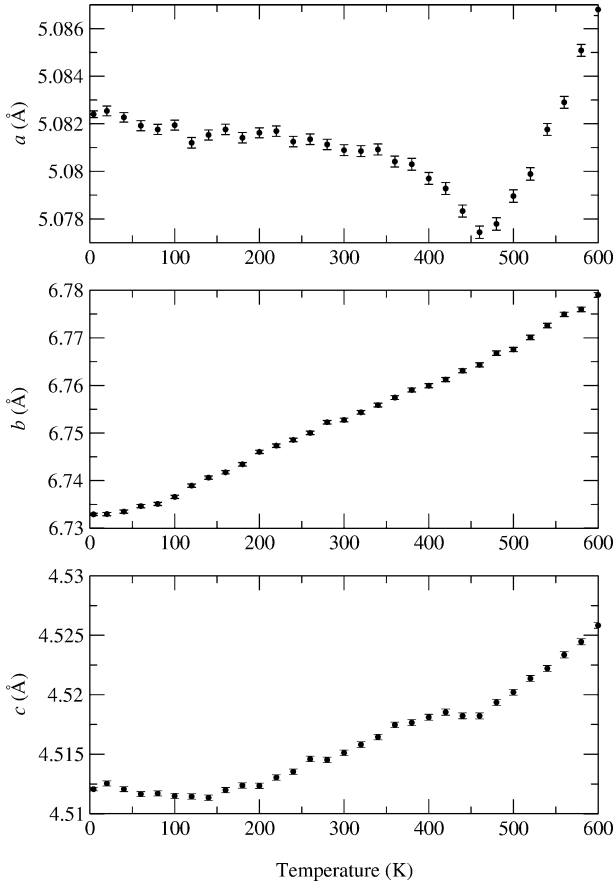

Figure 2
Lattice parameters of Fe_3C as a function of temperature; the error bars shown are at ± 1 the estimated standard uncertainty.

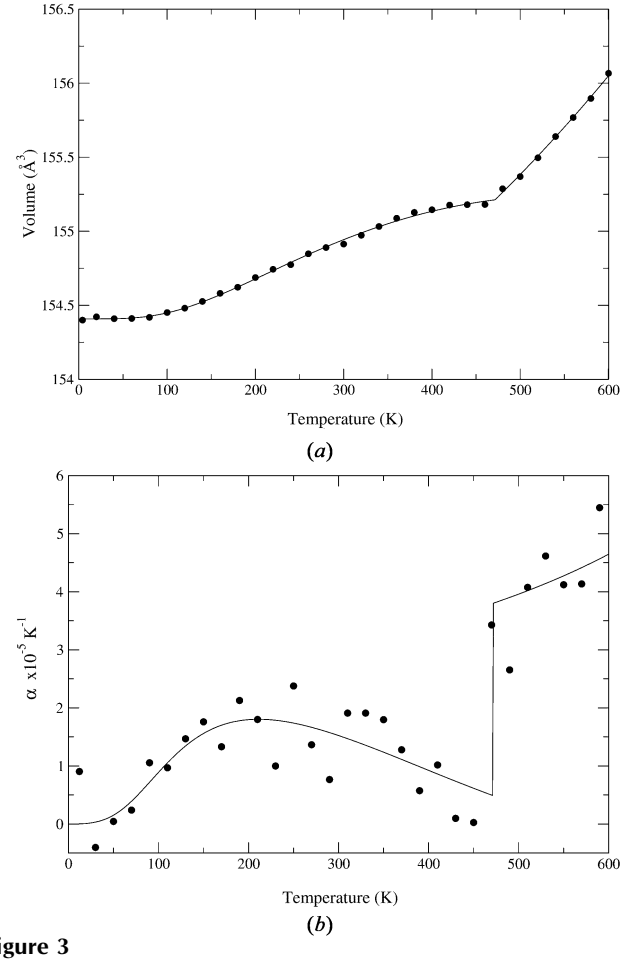

Figure 3
(*a*) Unit-cell volume of Fe_3C as a function of temperature. The symbols show the measured data points (the estimated standard uncertainties lie within the symbols). The line shows the results of the fit to equation (4). (*b*) Volumetric thermal expansion coefficient of Fe_3C as a function of temperature. The symbols were obtained by numerical differentiation of the data shown in (*a*). The line was obtained *via* equation (4).

If equation (1) is fitted to the eight data points above 460 K assuming, instead, that α is temperature independent, *i.e.* putting

$$\alpha(T) = \alpha_o, \tag{3}$$

we obtain α_o = 4.1 (1) $\times$ 10^{-5} K^{-1} and V_{T_r} = 154.14 (5) Å^3, again for T_r = 300 K.

It should be noted that these values of α are similar to that for α-Fe at these temperatures (α for α-Fe = 4.5 $\times$ 10^{-5} K^{-1} at 600 K; Krishnan *et al.*, 1979; Basinski *et al.*, 1955) but are somewhat higher than that used by Wood (1993), who adopted a value of 3.35 $\times$ 10^{-5} K^{-1} (based on Gachon & Schmitt, 1971) in his discussion of the possibility of Fe_3C forming a major component of the inner core of the Earth.

In previous recent studies of geologically important materials and their analogues (Vočadlo, Knight *et al.*, 2002*a*; Wood *et al.*, 2002), we have extended our analysis of thermal expansion data by fitting Grüneisen approximations to the zero-pressure equation of state (see Wallace, 1998) so as to obtain estimates of such quantities as the Debye temperatures and Grüneisen parameters. In the present case of Fe_3C, the behaviour of $V(T)$ is more complex than that considered previously because of the magnetic phase transition. We assume that the 'structural', $V_G(T)$, and 'magnetic', $V_M(T)$, contributions to the thermal expansion may be separated, *i.e.* that

$$V(T) = V_G(T) + V_M(T), \tag{4}$$

where $V_M(T) = 0$ for $T > T_c$. In order to model the non-linear temperature dependence of $V(T)$ above T_c (see below), it was found to be necessary to use a third-order Grüneisen approximation of the form (Wallace, 1998)

$$V_G(T) = V_o U/(Q - bU + cU^2) + V_o, \tag{5}$$

where $Q = V_o K_o/\gamma'$, $b = (K_o' - 1)/2$ and $c = (\gamma'/12K_oV_o)[2K_oK_o'' - (K_o')^2 + 6K_o' - 5]$; γ' is a Grüneisen parameter (assumed constant), K_o, K_o' and K_o'' are the incompressibility and its first and second derivatives with respect to pressure, respectively, at $T = 0$, and V_o is the volume at $T = 0$. The internal energy, U, may be calculated using the Debye approximation (see *e.g.* Cochran, 1973) from

$$U(T) = 9Nk_BT(T/\theta_D)^3 \int_0^{\theta_D/T} x^3\,dx/[\exp(x) - 1], \tag{6}$$

where N is the number of atoms in the unit cell, k_B is Boltzmann's constant and θ_D is the Debye temperature [note that the effect of the vibrational zero-point energy, $9Nk_B\theta_D/8$, is included in equation (5) *via* the term V_o and hence excluded from $U(T)$, since equation (5) requires that $U = 0$ at $T = 0$].

No detailed study of the temperature dependence of the spontaneous magnetization in Fe_3C has been reported. In order to obtain a description of $V_M(T)$ covering the complete range of reduced temperature below the transition while requiring the least number of adjustable parameters, it was assumed, therefore, that: (i) a simple mean-field model would be adequate to describe the evolution of the reduced spontaneous magnetization, $M_S(T)$, and (ii) the 'magnetic' contribution to the volume was proportional to M_S^2 (Shiga, 1981). Thus,

$$V_M(T) = A[M_S(T)]^2, \tag{7}$$

where A is a constant. The steps necessary to obtain $M_S(T)$, which are well known and therefore not discussed in detail here, are described by, for example, Blundell (2001); in essence, it is necessary to find numerical solutions to two simultaneous equations for the magnetization, the first being a Brillouin function $B_J(y)$ and the second being a straight line with slope proportional to temperature. In this way, it is possible to describe $V_M(T)$ in terms of only two adjustable parameters: the constant of proportionality, A, and the transition temperature, T_c. It is, of course, well known that mean-field models do not provide very accurate descriptions of $M_S(T)$, either close to T_c, where critical fluctuations will dominate the behaviour, or at low temperatures, where spin-wave quantization becomes important. Nevertheless, we believe that this model, which has the advantage of requiring only two adjustable parameters, is adequate for the present purposes. The Brillouin function adopted was $B_{1/2}(y)$ as it was known that this value of J gave the best fit to the magnetization curve for Fe and other ferromagnetic transition elements (Dekker, 1964). The limitations of equation (7) have been discussed by Shiga (1981), who suggested an alternative, more complex expression incorporating also the temperature-dependence of the local atomic magnetic moments.

The solid line in Fig. 3(*a*) shows the result obtained from fitting the data to equation (4); it can be seen that the fit to the data is good over the full temperature range of the experiment, although there is possibly insufficient curvature in the region immediately below T_c. In principle, this fit requires seven adjustable parameters (θ_D, Q, V_o, b, c, A and T_c). As might be expected from the form of equation (5), however, allowing both b and c to vary freely led to values with very large standard uncertainties and it was, therefore, decided to fix the value of b at 3/2, corresponding to a value of $K_o' = 4$. The alternative approach of fixing $c = 0$, *i.e.* using a second-order Grüneisen approximation for $V_G(T)$, gave an essentially identical fit to the data but required a value of b equivalent to $K_o' = 27$ (4), probably too large to be physically sensible. This is a consequence of the condition that the observed non-linear behaviour of the $V(T)$ data for $T > T_c$ can only be modelled by reduction of the denominator in equation (5). A similar, unacceptably high value of K_o' also resulted when the parameters b and c were constrained *via* the relationship between K_o' and K_o'' implicit in the Birch–Murgnahan third-order equation of state (see below).

The resulting values of the six fitted parameters were: θ_D = 604 (44) K, Q = 1.9 (2) $\times$ 10^{-17} J, V_o = 153.60 (2) Å^3, c = -2.7 (9) $\times$ 10^{19} J^{-1}, A = 0.81 (6) Å^3 and T_c = 472 (3) K. The line shown in Fig. 3(*b*) gives the corresponding behaviour of the thermal expansion coefficient, $\alpha(T)$, defined as

$$\alpha(T) = (1/V)(dV/dT), \tag{8}$$

obtained by differentiation of equation (4); it can be seen that this corresponds well with the data points shown in the figure,

which were determined by simple numerical differentiation by differences of the $V(T)$ data.

The Debye temperature of Fe_3C estimated from the fit to equation (4), 604 (44) K, would appear to be physically sensible, being, as might be expected, somewhat higher than that for pure iron (474 K; Poirier, 1991). Similarly, the value of T_c for the magnetic transition, 472 (3) K, is in agreement with that previously determined by Tsuzuki *et al.* (1984), 483 ± 5 K, from measurements of magnetization. The value of V_o, 153.60 (2) Å^3, corresponds to the volume that the unit cell of the paramagnetic phase of Fe_3C with disordered local magnetic moments would occupy if such a phase persisted to zero temperature. This is significantly higher than that obtained from first-principles calculations for 'non-magnetic' Fe_3C with no local magnetization [143.5 (1) Å^3; Vočadlo, Brodholt *et al.*, 2002]. However, we would not expect these two volumes to be the same since the introduction of local magnetic moments will significantly inflate the structure. This effect has been discussed by Shiga (1981), who suggested that a volume change of similar size would be expected between ferromagnetic and hypothetical 'non-magnetic' phases of body-centred cubic (b.c.c.) Fe. A limitation of the simple model of ferromagnetism used in equation (4) is that it assumes that the local magnetic moment does not vary with temperature. In practice, this may not be true, but we would not anticipate the variation to be significant over the temperature range of our experiment. With this proviso, we would expect our analysis to be representative of the properties of 'non-magnetic' Fe_3C under our experimental conditions.

The limitations of our model may well be responsible for the numerically large value of the parameter c, $-2.7\ (9) \times 10^{19}$ J^{-1}; by substituting the values of Q ($= V_oK_o/\gamma'$) and K_o' (= 4) in the relationship $c = (\gamma'/12K_oV_o)[2K_oK_o'' - (K_o')^2 + 6K_o' - 5]$ we obtain $K_oK_o'' = -3080\ (1100)$. This product is much higher than that which results from the implied values of K_o'' in many of the commonly used isothermal equations of state (see *e.g.* Angel, 2000), although the large standard uncertainty of the value of c means that the difference is not entirely outside the possible range of experimental error; for example, it is within three standard uncertainties of that required by the third-order Birch–Murnaghan equation where $K_oK_o'' = -[(3 - K_o')(4 - K_o') + 35/9] = -3.9$ for $K_o' = 4$.

It is interesting to discuss the results shown in Fig. 3(*b*) within the framework of the Ehrenfest classification of phase transitions (see *e.g.* Pippard, 1981). The behaviour of the thermal expansion coefficient derived *via* equation (4) is exactly that required at an Ehrenfest second-order transition: a second derivative of the Gibbs energy, $\alpha(T)$, is discontinuous at the phase boundary. This is to be expected, as the Weiss theory of ferromagnetism, which underlies equation (7), provides an example of a transition that is truly second order as defined by Ehrenfest. Real systems rarely show this ideal behaviour and thus, although the data points in Fig. 3(*b*) also show an apparent discontinuity at T_c, it is probable that a more precise and detailed study of the lattice parameters would reveal a more λ-like behaviour of the measured expansion coefficient (see *e.g.* Pippard, 1981).

An equation equivalent to the familiar Clapeyron equation for discontinuous transitions may be derived for transitions of second order. This takes the form (Pippard, 1981)

$$\mathrm{d}P/\mathrm{d}T = (\alpha_2 - \alpha_1)[(1/K_2) - (1/K_1)], \qquad (9)$$

where $\mathrm{d}P/\mathrm{d}T$ refers to the slope of the transition line and the subscripts denote, in the present case, the paramagnetic and ferromagnetic phases of Fe_3C, respectively. The value of the discontinuity in α at T_c obtained from the line shown in Fig. 3(*b*) is 3.33×10^{-5} K^{-1}. The change in the value of K across the ferromagnetic phase boundary has not been studied experimentally, but may be addressed *via* equation (9) if it is assumed that there is a linear phase boundary between the ferromagnetic and paramagnetic/'non-magnetic' phases. At ambient pressure, T_c = 483 K (Tsuzuki *et al.*, 1984) and the critical pressure at 0 K from first-principles calculations, P_c, is ∼60 GPa (Vočadlo, Brodholt *et al.*, 2002), giving a slope of -0.124 GPa K^{-1}. When combined with the value for $\alpha_2 - \alpha_1$ given above, these values lead to a denominator in equation (9) equal to -2.68×10^{-4} GPa^{-1}. If it is further assumed that the incompressibilities obtained by Scott *et al.* (2001) and Li *et al.* (2002) are still reasonably representative of ferromagnetic Fe_3C at T_c, *i.e.* $K_1 \simeq 175$ GPa, we can infer that K for the paramagnetic phase will be about 9 GPa higher. Perhaps surprisingly, the size of the discontinuity in K at P_c predicted by our recent first-principles calculations study (Vočadlo, Brodholt *et al.*, 2002) also leads to a value for the denominator in equation (9) almost identical to that given above. Using the equation-of-state parameters listed by Vočadlo, Brodholt *et al.* (2002), the incompressibilities at the volume at which the ferromagnetic phase transition occurs (7.9 Å^3 atom^{-1}) are found to be 531 GPa and 468 GPa for the 'non-magnetic' and ferromagnetic phases, respectively, thus leading to a difference in their reciprocals of -2.54×10^{-4} GPa^{-1}.

Finally, we may use the results above to make an estimate of the thermodynamic Grüneisen parameter, which is given by

$$\gamma_{\mathrm{th}} = \alpha K_T V/C_v, \qquad (10)$$

where K_T is the isothermal incompressibility and C_v is the specific heat at constant volume. Ignoring the contribution to C_v from the ferromagnetic transition (*i.e.* confining the discussion to temperatures well above T_c) and recalling that $C_v = \mathrm{d}U/\mathrm{d}T$, we obtain, by differentiating equation (5), the relationship

$$\gamma_{\mathrm{th}} = [(Q - cU^2)V_o/(Q - bU + cU^2)^2]K_T. \qquad (11)$$

At 600 K, we find that $\gamma_{\mathrm{th}} = 1.15 \times 10^{-11}K_T$. No measurements of the incompressibility of the paramagnetic phase of Fe_3C have yet been reported. Estimates of K_T at this temperature may be obtained either by using the equation of state given by Vočadlo, Brodholt *et al.* (2002), together with the value of the unit-cell volume at 600 K from the present study ($K_T \simeq$ 217 GPa) or, as discussed above, from the results of Scott *et al.* (2001) and Li *et al.* (2002) and equation (9) ($K_T \simeq 184$ GPa). The resulting values of γ_{th} are 2.5 and 2.1; although these are a little higher than commonly reported, they are similar to that obtained in a recent study of FeSi, $\gamma_{\mathrm{th}} = 2.1$, which was based

Table 1
Fractional coordinates and isotropic atomic displacement parameters of Fe_3C as a function of temperature.

The space group is *Pnma*, with the origin as in *International Tables for X-ray Crystallography* (1969). Fe1 atoms lie on general positions (8*d*); Fe2 and C atoms that lie on special positions on the mirror planes (4*c*) have coordinates *x*, 1/4, *z*. The displacement parameters of Fe1 and Fe2 were constrained to be equal in the refinement.

T (K)	Fe1 *x*	Fe1 *y*	Fe1 *z*	Fe2 *x*	Fe2 *z*	C *x*	C *z*	$100u_{Fe}$ (Å^2)	$100u_C$ (Å^2)
4.2	0.1841 (4)	0.0571 (3)	0.3329 (5)	0.0336 (5)	0.8409 (8)	0.8942 (9)	0.4503 (8)	1.4 (1)	4.1 (2)
20	0.1844 (4)	0.0565 (4)	0.3321 (5)	0.0332 (5)	0.8410 (9)	0.8937 (10)	0.4494 (9)	1.3 (1)	3.8 (2)
40	0.1838 (4)	0.0567 (4)	0.3326 (5)	0.0330 (5)	0.8407 (9)	0.8941 (10)	0.4500 (9)	1.7 (1)	4.1 (2)
60	0.1836 (4)	0.0571 (4)	0.3322 (5)	0.0335 (5)	0.8401 (9)	0.8944 (10)	0.4487 (9)	1.4 (1)	4.0 (2)
80	0.1842 (4)	0.0567 (4)	0.3322 (5)	0.0336 (5)	0.8410 (9)	0.8924 (10)	0.4490 (9)	1.3 (1)	3.8 (2)
100	0.1835 (4)	0.0579 (4)	0.3337 (5)	0.0339 (5)	0.8381 (9)	0.8950 (10)	0.4485 (9)	1.3 (1)	3.6 (2)
120	0.1837 (4)	0.0575 (4)	0.3330 (6)	0.0342 (5)	0.8386 (9)	0.8947 (10)	0.4484 (10)	1.4 (1)	3.8 (2)
140	0.1843 (4)	0.0577 (4)	0.3328 (6)	0.0342 (5)	0.8403 (9)	0.8954 (10)	0.4495 (9)	1.3 (1)	3.8 (2)
160	0.1840 (4)	0.0581 (4)	0.3332 (6)	0.0344 (5)	0.8393 (9)	0.8961 (10)	0.4479 (9)	1.4 (1)	3.9 (2)
180	0.1840 (4)	0.0576 (4)	0.3325 (6)	0.0343 (5)	0.8394 (10)	0.8963 (11)	0.4496 (9)	1.4 (1)	3.9 (2)
200	0.1844 (4)	0.0574 (4)	0.3319 (6)	0.0344 (5)	0.8390 (9)	0.8957 (10)	0.4488 (9)	1.5 (1)	3.8 (2)
220	0.1842 (4)	0.0579 (4)	0.3323 (6)	0.0341 (5)	0.8405 (10)	0.8949 (10)	0.4493 (9)	1.6 (2)	3.8 (2)
240	0.1843 (4)	0.0584 (4)	0.3322 (6)	0.0343 (5)	0.8388 (10)	0.8959 (10)	0.4494 (9)	1.7 (2)	3.4 (2)
260	0.1844 (5)	0.0585 (4)	0.3325 (6)	0.0348 (5)	0.8388 (10)	0.8982 (10)	0.4491 (9)	1.4 (1)	3.2 (2)
280	0.1843 (5)	0.0589 (4)	0.3336 (6)	0.0349 (5)	0.8378 (10)	0.8979 (10)	0.4474 (9)	1.5 (1)	3.3 (2)
300	0.1846 (5)	0.0594 (4)	0.3340 (6)	0.0346 (6)	0.8377 (10)	0.8984 (10)	0.4467 (9)	1.2 (1)	2.9 (2)
320	0.1845 (5)	0.0584 (4)	0.3330 (6)	0.0347 (6)	0.8373 (10)	0.8974 (10)	0.4502 (9)	1.4 (1)	2.8 (2)
340	0.1844 (5)	0.0592 (4)	0.3343 (6)	0.0345 (6)	0.8362 (10)	0.8982 (10)	0.4488 (9)	1.6 (2)	2.8 (2)
360	0.1855 (5)	0.0593 (4)	0.3331 (6)	0.0353 (6)	0.8368 (10)	0.9008 (10)	0.4483 (9)	1.4 (1)	2.3 (2)
380	0.1845 (5)	0.0592 (4)	0.3347 (6)	0.0350 (6)	0.8355 (10)	0.8997 (10)	0.4495 (9)	1.8 (2)	2.6 (2)
400	0.1863 (5)	0.0587 (4)	0.3323 (6)	0.0353 (6)	0.8378 (10)	0.8987 (10)	0.4504 (9)	1.6 (2)	2.4 (2)
420	0.1862 (5)	0.0593 (4)	0.3328 (6)	0.0352 (6)	0.8357 (11)	0.9016 (10)	0.4482 (9)	1.5 (2)	2.1 (3)
440	0.1858 (5)	0.0593 (4)	0.3341 (6)	0.0356 (6)	0.8338 (10)	0.9015 (10)	0.4495 (9)	1.6 (2)	1.8 (2)
460	0.1865 (5)	0.0595 (4)	0.3344 (6)	0.0349 (6)	0.8344 (11)	0.9011 (10)	0.4488 (9)	1.6 (2)	1.5 (2)
480	0.1874 (5)	0.0590 (4)	0.3323 (6)	0.0348 (6)	0.8361 (11)	0.9024 (11)	0.4490 (9)	1.5 (2)	1.7 (3)
500	0.1886 (5)	0.0589 (4)	0.3321 (6)	0.0354 (6)	0.8373 (11)	0.9021 (11)	0.4491 (9)	1.6 (2)	1.5 (3)
520	0.1884 (5)	0.0588 (5)	0.3330 (6)	0.0348 (6)	0.8350 (11)	0.9036 (11)	0.4485 (9)	1.6 (2)	1.3 (3)
540	0.1883 (5)	0.0579 (4)	0.3320 (6)	0.0340 (6)	0.8355 (11)	0.9045 (11)	0.4491 (9)	2.0 (2)	1.8 (3)
560	0.1895 (5)	0.0585 (5)	0.3319 (6)	0.0342 (7)	0.8352 (11)	0.9045 (11)	0.4480 (9)	1.9 (2)	1.4 (3)
580	0.1902 (5)	0.0573 (5)	0.3307 (6)	0.0342 (7)	0.8388 (12)	0.9049 (11)	0.4490 (10)	2.2 (2)	1.9 (3)
600	0.1905 (6)	0.0572 (5)	0.3314 (7)	0.0345 (7)	0.8371 (12)	0.9060 (11)	0.4481 (10)	2.3 (2)	1.6 (3)

on experimental measurements of all four quantities involved (Vočadlo, Knight *et al.*, 2002).

3.2. Magnetic structure

In general, we would expect the effect of ferromagnetic order on the intensities of the Bragg reflections in the neutron powder diffraction pattern of Fe_3C to be small as the nuclear scattering in this material is strong; thus, we might expect unambiguous determination of the ferromagnetic structure solely from powder data to be very difficult. For Fe_3C, the onset of ferromagnetism need not be associated with a change in crystal class. The point group of Fe_3C is *mmm*; when time-reversal symmetry is also allowed, there are eight corresponding magnetic groups. Ferromagnetism is allowed in three, namely *mm′m′*, *m′mm′* and *m′m′m* (where the prime signifies the time reversal operation), with the bulk magnetization directed perpendicular to the ordinary mirror plane, *i.e.* parallel to *a*, *b* and *c*, respectively. Careful examination of the diffraction patterns above and below T_c did not reveal any additional peaks, and so there was no indication that the magnetic unit cell is different from the crystallographic unit cell. The magnetic space groups that are consistent with this observation are *Pnm′a′*, *Pn′ma′* and *Pn′m′a*. There are two distinct Fe sites in the unit cell; Fe1 sits on a general position and Fe2 sits on the mirror plane (see below). The magnetic moment of Fe1 is not constrained by symmetry to lie in any fixed direction; that of Fe2 must be directed parallel to [010] in space group *Pn′ma′*, while in space groups *Pnm′a′* and *Pn′m′a* it must lie in (010). Inspection of the axial ratios across the magnetic transition (see below) suggested that the bulk magnetization might be directed along [100] and thus that *Pnm′a′* is the most likely space group. Rietveld refinements were carried out in all three possible space groups using both data sets previously collected on POLARIS at 300 K (Vočadlo, Brodholt *et al.*, 2002) and HRPD data at 4.2 K (present study). For the POLARIS data, the magnetic moments of both Fe atoms were initially fixed parallel to the appropriate bulk magnetization direction; very similar values of χ^2 were obtained for all three space groups, $2.9 < \chi^2 < 3.1$ (47 variables), whereas in the non-magnetic refinement, $\chi^2 = 3.1$ (45 variables). Further attempts to refine the magnetic structure in *Pnm′a′* without fixing the direction of the magnetic moment did not lead to any improvement. Similar inconclusive results were obtained from the HRPD data at 4.2 K. It appears, therefore, that our present experiments are insufficient to determine the magnetic structure of Fe_3C.

3.3. Crystal structure

The fractional coordinates and isotropic atomic displacement parameters at all measured temperatures, with the

crystallographic structure refined in space group *Pnma*, are shown in Table 1. As we were unable to determine the magnetic structure, this component of the scattering could not be included in the refinement. Comparison of our results at 300 K with those of Herbstein & Smuts (1964; refinement from X-ray powder data from Fe_3C) shows no differences in coordinates that can be regarded as significant; the majority differ by less than one standard uncertainty of the difference and the largest discrepancy (in C z) is less than 3.5 standard uncertainties. The agreement with Fasiska & Jeffrey (1965; single-crystal X-ray refinement from a sample of composition $Fe_{2.7}Mn_{0.3}C$) is less good but still satisfactory, bearing in mind that it will reflect, at least in part, real differences arising from the different chemical composition of the samples. For the Fe atoms, which are well determined in both refinements, the largest difference is that for the y coordinate of Fe1 [0.0072 (4) Å]. The x coordinate of the C atom differs by a numerically greater amount [0.021 (3) Å], but this can probably be attributed to the relatively poor determination of the C-atom positions in the X-ray study.

It is clear, however, from Table 1 that the behaviour of the isotropic displacement parameter of the carbon atom, which falls smoothly from a value of about 0.04 Å^2 at 4.2 K to ~0.015 Å^2 at and above T_c, is not physically sensible. The most likely explanation for this behaviour would seem to lie in our neglect of the magnetic component of the scattering of the Fe atoms. Thus, although comparisons with previous work show that our structures are not grossly in error, we believe that the accuracy of our coordinates is probably somewhat less than might be supposed on the basis of their estimated standard uncertainties and this suggests that caution should be exercised when considering the effects of temperature on the structure. The changes in the values of all of the coordinates between 4 K and 600 K are slight. Although apparently systematic trends are observed in some cases, for example, in the x coordinates of Fe1 and C, the span of the values is similar to the differences between our refinement and the results of Fasiska & Jeffrey (1965). None of the five Fe fractional coordinates changes by more than 0.007 across the full temperature range; the C z coordinate is similarly invariant, with the C x coordinate (the largest shift in the structure) changing by 0.012.

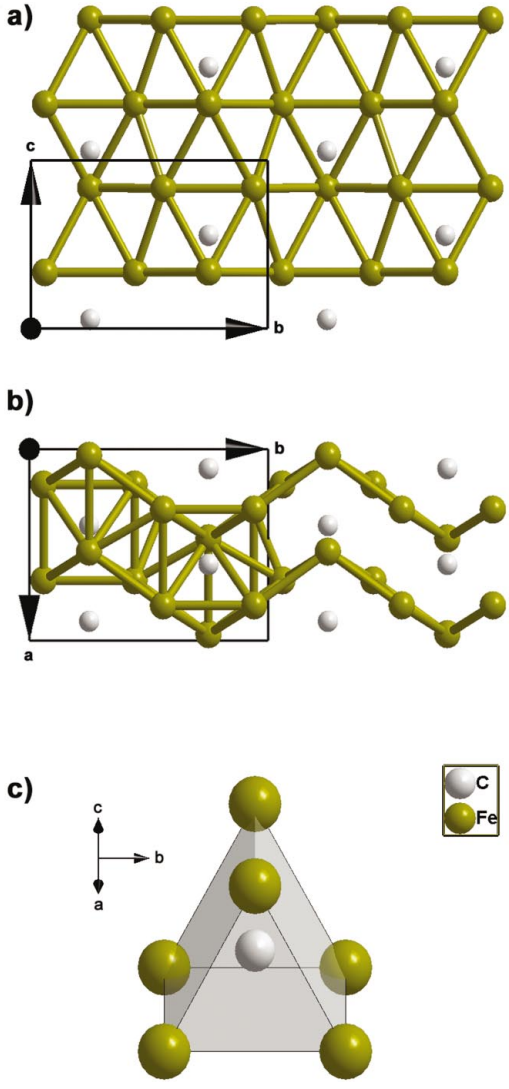

Figure 4
(*a*) Projection of the cementite structure down [100]. Only those atoms with fractional coordinates in the range $0 < x < 0.5$ are shown, corresponding to a single close-packed pleated sheet of Fe atoms. (*b*) Projection of the cementite structure down [001], showing the pleating of the close-packed sheets of Fe atoms; the inter-sheet Fe–Fe contacts are shown in the left-hand half of the diagram. (*c*) Local environment of a C atom, viewed down [101], showing the trigonal prismatic coordination by six Fe atoms.

Detailed discussions of the cementite structure have been presented by Fasiska & Jeffrey (1965) and by Hyde & Andersson (1989). Since the present study shows it to be almost temperature invariant, we shall confine ourselves to a few brief remarks. Cementite is possibly most easily viewed as being derived from a hexagonal close-packed array of Fe atoms. The close-packed sheets are, however, not flat but 'pleated', an arrangement which Hyde & Andersson (1989) discuss in terms of repeated twinning. Figs. 4(*a*) and 4(*b*) give projections of the structure viewed down the *a* and *c* axes, respectively (*i.e.* perpendicular and parallel to the plane of the pleated sheets). The folds of the pleats coincide with the mirror planes in the structure at $y = 1/4, 3/4$ (Fig. 4*b*). Fe atoms on special positions, Fe2, sit on the mirror planes and thus lie along the ridges of the folds. The pleated close-packed sheets lie parallel to (100) and are separated in the unit cell by $a/2$. The carbon atoms also sit on the mirror planes, directly above the fold lines, and are coordinated by six Fe atoms in a fairly regular trigonal prism, as shown in Fig. 4(*c*). The Fe atoms in general positions, Fe1, are 11-fold coordinated by Fe atoms, whereas Fe2 is 12-fold coordinated by Fe. In the case of Fe1, the arrangement of nearest neighbours is similar to that observed in normal hexagonal close packing (with one C atom completing the 12-fold coordination); the coordination of Fe2 is more irregular.

Inspection of the axial ratios suggests that the structural consequences of the ferromagnetic transition mainly involve the *a* axis: while b/a and c/a show a marked break in slope at

T_c, c/b does not. The largest change in fractional coordinate with temperature is that of C x, corresponding to a shift of approximately 0.07 Å in a direction perpendicular to the pleated sheets. The four distinct C—Fe bond distances in the trigonal prism change from 1.905 (6), 2.041 (6), 2.063 (6) and 2.109 (5) Å at 20 K, to 1.879 (7), 2.021 (6), 2.126 (7) and 2.124 (5) Å at 600 K, respectively, with the C atom thus occupying a slightly less central position in its coordination polyhedron as the temperature increases. Similar subtle changes are observed in some Fe—Fe distances; even the largest variation, however, amounts to only 0.06 Å and in most cases the changes are much less. A final quantity of interest is the angle at which the pleated sheets are folded. Since the Fe2 atoms lie along the hinge lines of the folds, the folding angle is given by $2\tan^{-1}[b/a(1 - 4x_{Fe2})]$; again, this angle is almost temperature independent, varying from about 113.6° at 4.2 K to a maximum of 114.35° around T_c.

4. Conclusions

We have shown that the volumetric thermal expansion coefficient of cementite is very temperature dependent, with the material showing a strong 'Invar effect'. When modelling the Earth's interior, it is, therefore, essential that values appropriate to the high-pressure high-temperature phase of Fe_3C are used. Over the temperature range examined, the behaviour of the material may be adequately described by a Grüneisen approximation to the zero-pressure equation of state, combined with a model of the magnetostriction based on mean-field theory. Within the limitations of our structure refinements, no obvious change in the crystal structure can be seen on passing from the paramagnetic to the ferromagnetic phase.

LV and JB gratefully acknowledge receipt of Royal Society University Research Fellowships; DPD is grateful to the Alexander von Humboldt Stiftung for a Visiting Fellowship. Financial support for the experiment was also provided by NERC. We would also like to thank H. Vočadlo for his assistance during the experiments and A. D. Fortes and M. J. Gillan for helpful discussions.

References

Angel, R. J. (2000). *Review of Mineralogy and Geochemistry*, Vol. 41, *High-Temperature and High-Pressure Crystal Chemistry*, edited by R. M. Hazen & R. T. Downs, pp 35–59. Washington: Mineralogical Society of America.

Basinski, Z. S., Hume-Rothery, W. & Sutton, A. L. (1955). *Proc. R. Soc. Ser. A*, **229**, 459–467.

Blundell, S. (2001). *Magnetism in Condensed Matter.* Oxford University Press.

Brown, P. J. & Matthewman, J. C. (1993). Report RAL-93-009, Rutherford Appleton Laboratory, Oxford.

Cochran, W. (1973). *The Dynamics of Atoms in Crystals.* London: Arnold.

Dekker, A. J. (1964). *Solid State Physics.* London: Macmillan.

Fasiska, E. J. & Jeffrey, G. A. (1965). *Acta Cryst.* **19**, 463–471.

Fei, Y. (1995). *AGU Reference Shelf 2: Mineral Physics and Crystallography – A Handbook of Physical Constants*, edited by T. J. Ahrens, pp. 29–44. Washington: AGU.

Gachon, J. C. & Schmitt, B. (1971). *C. R. Acad. Sci. Paris Sér. C*, **272**, 428–431.

Häglund, J., Grimvall, G. & Jarlborg, T. (1991). *Phys. Rev. B*, **44**, 2914–2919.

Herbstein, F. H. & Smuts, J. (1964). *Acta Cryst.* **17**, 1331–1332.

Hofer, L. J. E. & Cohn, E. M. (1959). *J. Am. Chem. Soc.* **81**, 1576–82.

Hyde, B. G. & Andersson, S. (1989). *Inorganic Crystal Structures*. New York: Wiley.

Ibberson, R. M., David, W. I. F. & Knight, K. S. (1992). Report RAL-92-031, Rutherford Appleton Laboratory, Oxford.

International Tables for X-ray Crystallography (1969). Vol. I. Birmingham: Kynoch Press.

Kohlhaas, R., Dünner, Ph. & Schmitz-Pranghe, N. (1967). *Zeit. Angew. Phys.* **23**, 245–249.

Krishnan, R. S., Srinivasan, R. & Devanarayanan, S. (1979). *Thermal Expansion of Crystals*. Oxford: Pergamon.

Larson, A. C. & Von Dreele, R. B. (1994). *GSAS* (*General Structure Analysis System*). Report LAUR 86-748, Los Alamos National Laboratory.

Li, J., Mao, H. K., Fei, Y., Gregoryanz, E., Eremets, M. & Zha, C. S. (2002). *Phys. Chem. Miner.* **29**, 166–169.

Pawley, G. S. (1981). *J. Appl. Cryst.* **14**, 357–361.

Pippard, A. B. (1981). *The Elements of Classical Thermodynamics.* Cambridge University Press.

Poirier, J. P. (1991). *Introduction to the Physics of the Earth's Interior*. Cambridge University Press.

Reed, R. C. & Root, J. H. (1998). *Scr. Materialia*, **1**, 95–99.

Scott, H. P., Williams, Q. & Knittle, E. (2001). *Geophys. Res. Lett.* **28**, 1875–1878.

Shiga, M. (1981). *J. Phys. Soc. Jpn*, **50**, 2573–2580.

Tsuzuki, A., Sago S., Hirano, S. & Naka S. (1984). *J. Mater. Sci.* **19**, 2513–2518.

Vočadlo, L., Brodholt, J., Dobson, D., Knight, K. S., Marshall, W., Price, G. D. & Wood, I. G. (2002). *Earth Planet. Sci. Lett.* **203**, 567–575.

Vočadlo, L., Knight, K. S., Price, G. D. & Wood, I. G. (2002*a*). *Phys. Chem. Miner.* **29**, 132–139.

Wallace, D. C. (1998). *Thermodynamics of Crystals.* New York: Dover.

Wood, B. J. (1993). *Earth Planet. Sci. Lett.* **117**, 593–607.

Wood, I. G., Knight, K. S., Price, G. D. & Stuart, J. A. (2002). *J. Appl. Cryst.* **35**, 291–295.